

Article

Not peer-reviewed version

Designing A Dispatch Engine for Hybrid Renewable Power Station Using Mixed-Integer Linear Programming (MILP) Technique

Myada Shadoul , [Rashid Al Abri](#) , [Hassan Yousef](#) ^{*} , Abdullah Al Shereiqi

Posted Date: 13 May 2024

doi: 10.20944/preprints202405.0865.v1

Keywords: Hybrid renewable energy system (HRES); Optimization; Dispatch Engine (DE); Mixed Integer Linear Programming (MILP); Feed-Forward Neural Networks (FFNN); Forecasting.



Preprints.org is a free multidiscipline platform providing preprint service that is dedicated to making early versions of research outputs permanently available and citable. Preprints posted at Preprints.org appear in Web of Science, Crossref, Google Scholar, Scilit, Europe PMC.

Copyright: This is an open access article distributed under the Creative Commons Attribution License which permits unrestricted use, distribution, and reproduction in any medium, provided the original work is properly cited.

Article

Designing A Dispatch Engine for Hybrid Renewable Power Station Using Mixed-Integer Linear Programming (MILP) Technique

Myada Shadoul ¹, Rashid Al Abri ^{1,2}, Hassan Yousef ^{2,*} and Abdullah Al Shereiqi ¹

¹ Sustainable Energy Research Center, Sultan Qaboos University, Muscat-123, Oman

² Department of Electrical and Computer Engineering, Sultan Qaboos University, Muscat-123, Oman

* Correspondence: hyousef@squ.edu.om

Abstract: Hybrid power plants have recently emerged as reliable and flexible electricity generation stations by combining multiple renewable energy sources, energy storage systems (ESS), and fossil-based output. However, the effective operation of the hybrid power plants to ensure continuous energy dispatch under challenging conditions is a complex task. This paper proposes a dispatch engine (DE) based on mixed-integer linear programming (MILP) for the planning and management of hybrid power plants. To maintain the committed electricity output, the dispatch engine will provide schedules for operation over extended time periods as well as monitor and reschedule the operation in real-time. Through precise prediction of the Load, PV and wind power output, the proposed approach guarantees optimum scheduling. The precise prediction of the Load, PV and wind power are achieved by employing a predictor of Feed-Forward Neural Network (FFNN) type. With such a dispatch engine, the operational cost of the hybrid power plants, and the use of diesel generators (DGs) are both minimized. A case study is carried out to assess the proposed dispatch engine feasibility. A real-time measurement data pertaining to load, wind, and PV power outputs is obtained from different locations in the Sultanate of Oman. The real-time data is utilized to predict the future output power from PV and the Wind farm over 24 hours. The predicted powers are then used in combination with a PV-Wind-DG-ESS-Grid hybrid plant to evaluate the performance of the proposed dispatch engine. The proposed approach is implemented and simulated using MATLAB. The results of the simulation reveal the proposed Feed-Forward Neural Network's (FFNN) powerful forecasting abilities. In addition, the results demonstrate that adopting the proposed DE can minimize the use of DG units and reduce plant running expenses.

Keywords: hybrid renewable energy system (HRES); optimization; dispatch engine (DE); mixed Integer Linear programming (MILP); feed-forward neural networks (FFNN); forecasting

1. Introduction

The use of renewable energy (RE) sources has increased recently to reduce the need for fossil fuels and minimize the carbon footprint of electrical power systems [1]. By its very nature, renewable energy is a sustainable resource that may, over time, reduce the cost of energy generation and increase energy security. The cost of RE generation has decreased as a result of recent advances in RE technology, and the integration of RE sources into current power systems has increased significantly [1].

Two accessible renewable energy sources that can be used to produce clean electricity are solar and wind. Recent technology developments have made it possible to harvest power from solar and wind energy installations more cheaply and efficiently [1]. The validity of these sources is a significant question, though. Because wind speed varies, it is impossible to harness all of it. Similar to how solar irradiation varies during the day, no electricity is produced at night due to the

unpredictable nature of solar irradiation [2]. The main difficulties for system operators are variability and ramp events in output power, reserve management, scheduling, and commitment of generating units. As a consequence, wind and PV sources are non-dispatchable. The challenges brought on by the intermittent nature of these sources must be removed in order to integrate RE sources into the main power system. To provide acceptable electric dependability and power quality, substantial storage systems and traditional backup production must be included due to the non-dispatchable and intermittent nature of RE sources [3]. The electricity produced by wind and solar power plants may be combined, and a dispatchable power producing station can be constructed, with the right size of the energy storage systems (ESS). By storing the surplus produced power in the ESS and discharging the ESS when the production of RE sources decreases, a hybrid power plant with ESS made up of numerous RE sources may offer a reliable power supply. A cost-effective microgrid design and the development of intelligent management systems that can integrate the operation of various energy sources are required due to the growing system complexity [4]. With a suitable energy management system and well-designed control structure, a hybrid wind-PV-ESS power plant may remove the fluctuations of the wind-PV power and so constitute a dispatchable RE source, improving system dependability, lowering supply intermittency, and enhancing system security.

An electrical system is referred to as a hybrid renewable energy system (HRES), which combines one renewable energy source with a number of other energy sources. These sources may be conventional, sustainable, or a combination of both, and the system may be utilized independently or as part of a grid [5]. At the point of common coupling (PCC), the generating station must produce a consistent amount of electricity for the power utilities. There are severe consequences that the electricity producing firm must bear for any departure from earlier commitments. There is a need to install an emergency power source in case of failure to provide electricity owing to lower output from PV and wind generators in order to prevent any expensive penalties. During such crises, electricity can be provided by a diesel or gas-powered generator. As a result, a dependable hybrid power plant has to have RE generation (wind and/or PV), an ESS, and a diesel or gas backup emergency power supply.

Numerous studies for distant off-grid regions have shown that several hybrid energy system types are cost-effective generator combinations including PV/Wind, PV/Diesel, Wind/Diesel, and PV/Wind/Diesel with or without a storage device battery [6]. This was demonstrated in [7] which examined the techno-economic viability of a hybridized PV/Wind/Diesel/Batt system for a large non-residential power application. The authors of [7] stated that a carbon price policy and lower lending rate may support the sizable renewable energy-based project. An ideal hybridized system according to technological, economic, and environmental variables was presented in [8]. The study in [9] looked at the viability of a PV/Wind/Batt/Diesel system for illuminating a rural place. Comparing the hybrid system to the standard power generating system, the study found that the hybrid system is both economically and ecologically viable.

The energy management system in a microgrid is in charge of ensuring that it runs as efficiently as possible in the presence of probabilistic distributed generation units, interruptible loads, programmable distributed generation units, energy storage units, and ultimate consumers as the system's core [10]. A smart microgrid is employed in [11], and it is demonstrated that doing so not only boosts energy efficiency but also makes it possible to create a complementary and efficient network that may enhance dependability and power quality. Moreover [12] introduces a microgrid with an energy management center system, whose job it is to maximize the microgrid's performance in both island and grid-connected modes. Furthermore, research interest in evaluating the dispatch techniques and optimization algorithms of islanded microgrid has developed. The study in [2] assesses the optimal component sizes, power system responses, and various microgrid cost analyses to analyze the design and optimization of an island-based hybrid microgrid for various load dispatch techniques.

Economic Dispatch (ED), a form of energy management, aims to meet load demand while maintaining a minimal operational cost [13]. An effective ED approach may reduce resource usage and costs while also reducing the release of dangerous greenhouse gases [14]. Due to its efficiency,

ED technique in microgrid designing has become a popular topic in recent years [15]. Either a dispersed control approach or a centralized control strategy can be used to address issues with economic dispatch. The requirement for a bidirectional communication link between the centralized controller and all of the generating units under centralized control raises the cost, the risk of cyber-attack, and the complexity of communication. On the other hand, a distributed control method employs a dispersed controller that only manages a small region, resulting in a simpler control and communication network [16]. A unique distributed control approach based on the consensus method has been devised in [17,18] for the resolution of ED issues. In [18] The implemented technique forces the generators to learn about the imbalance between supply and demand. Each generator receives this estimated mismatch data, and as a result, the quantity of power generated is changed to account for the discrepancy. To account for the unpredictability in the generation of renewable energy, [19] proposes a real-time economic dispatch (RTED) approach together with a subinterval coordination technique for the conventional power plants. In [20] without taking into account communication networks, researchers demonstrated a two-level decentralized optimization strategy that facilitated power dispatch control approaches for an off-grid microgrid. In [21,22], in order to manage the high renewable penetration, authors designed a reliable energy distribution system using the distributed economic dispatch technique for a microgrid.

There have been many distinct two-layer models presented in the literature [23]. The majority of methods disentangle design and dispatch issues by using the fixed architecture systems' performance evaluation as a fitness metric to direct the exploration of the design space [24]. Mixed Integer Linear Programming (MILP) is a second-layer control technique that is more sophisticated and suitable for complex system topologies [25]. Utilizing future anticipated behavior of external elements (such as load and solar radiation) to determine the best solution and save operating costs, the MILP formulation employs powerful mathematical algorithms. The Author in [26] demonstrated for a rural ICE-BESS-PV microgrid, formal set points optimization can result in significant savings when compared to simpler heuristic solutions. The two-layer models have the disadvantage that they make it more difficult to include seasonal and annual constraints. Additionally, an iterative process is necessary for an accurate accounting of wearing costs for components whose lifetime is modified by their yearly shipment [27]. The Work in [27] presents an improved MILP-based predictive design and dispatch technique. The new approach is contrasted to an earlier heuristic methodology, using local microgrids' design and annual performance estimation as examples [27].

One way to formulate a complicated issue that may be solved with MILP is to combine in a single-layer model, the optimization of design and dispatch. For the optimization of geographically dispersed off-grid microgrids using solar panels and wind turbine generators, a more straightforward model is described in [28]. The model maximizes the quantity, location, and electrical connections between consumption sites, but it ignores the setup and administration of dispatchable generators. In [29], a MILP is used to optimize the design of a distributed multi-node CHP system with dispatchable and non-dispatchable DERs in both on-grid and off-grid situations.

An off-grid hybrid microgrid includes controllable and non-controllable generating units as well as a storage system, using a two-layer predictive management approach is presented in the study [30]. The second layer controls real-time operation and applies a response filter to tame variations in genset load while the higher layer deals with unit commitment. An actual rural microgrid in Somalia's data is used to evaluate the algorithm, which runs minute-by-minute simulations. Results are contrasted with a newly updated heuristic algorithm and the management technique that is currently in use. The two new techniques reduce fuel use by 15% compared to the prior management system [30]

Furthermore, sizing components and developing an efficient operation plan are essential steps in ensuring the competitiveness of off-grid systems in order to reduce the levelized cost of electricity (LCOE) for its consumers. Various strategies can be used, as shown in Table 1 [27].

Table 1. Sizing components strategies.

Model type	Analytical	Two layers	Single layer
Design identification (layer 1)	analytical expression	GA, PSO, Pattern search	MILP
Dispatch strategy (layer 2)	Simulation not performed	heuristic	MILP
		LF	
		CC	
		ABV	
		MILP	

Analytical models that just need assumptions on the total energy consumption and the technological capabilities of the various components can be used to estimate off-grid LCOE [31]. These models have the benefit of requiring extremely little computing time, and as a result, they are the technique of choice for estimating off-grid costs in early electrification planning studies. However, they do not specifically address the design and dispatch issue, which might result in an inaccurate LCOE calculation. More sophisticated simulation-based design methods that choose the size of components based on the predicted performance of potential solutions over a reference period can get around this restriction [27]. A quick and accurate method of replicating the operation of the microgrid is to use heuristic dispatch logics. Because of the state of the art in commercially available hardware, they consist of a set of established rules that regulate the system depending on its condition and the features of the installed equipment. They also have the advantage of being easily deployable in actual systems [27]. They are integrated into the popular HOMER simulation-based microgrid design optimization program [32].

The concept of optimization and optimization methods utilized for hybrid renewable power plant with several generation sources is required to dispatch electricity from each of the sources in accordance with the requirements stated by the operator or controller. Consequently, such a controller may also be referred to as a "Dispatch Engine (DE)" [33]. In order to ensure the necessary power flow through all devices, the DE for a hybrid power plant, which is a real-time control system must precisely and quickly handle various power sources and ESS [2].

A description of the sizes, energy, and power capacities of each system component whose design was predetermined is the primary output of an optimization process in a RES in its most basic form. A more complicated level of optimization is possible to carry out, such as real-time system reconfiguration by the controller (such as energy routing through electricity, hydrogen, or both), over a variety of potential configurations of the system's parts. To what extent a system will function and meet its technical and non-technical design objectives depends greatly on the component configuration and size choices made [34].

There are several objectives in a hybrid system that require optimization, including management, control, and sizing. The most popular optimization techniques employed in the past few years are listed in this section. The three categories of optimization techniques include classical techniques, artificial techniques, and hybrid techniques [35,36]. Table 2 summarized those used techniques.

Table 2. Optimization techniques for Hybrid renewable energy systems.

	Optimization techniques	Ref
Classic techniques [36]	The linear programming model (LPM)	[37,38]
	Multi choice goal programming (MCGP)	[39]
	Multi-objective evolutionary algorithms (MOEA)	[40,41]
	Mixed integer linear programming (MILP)	[27,42]
	Dynamic programming (DP)	[43]
	Nonlinear programming (NLP)	[44]
Artificial techniques	Fuzzy logic	[45–48]
	Genetic algorithm	[49–53]
	Neural network	[54,55]
	Particle swarm optimization (PSO)	[56–58]
Hybrid techniques		[34,59–64]

While several studies have explored hybrid renewable energy systems, optimization, and power forecasting techniques, none have specifically addressed a PV-DG-ESS-grid hybrid renewable energy systems with precise forecasting using real-time data, particularly in the context of Oman. Therefore, there is a research gap that needs to be addressed. The present paper introduces the Dispatch Engine (DE) as a solution to this gap, aiming to fill the aforementioned research void and examine the feasibility of implementing such a strategy in Oman. By incorporating real-time data and considering the unique operational conditions of Oman, the DE seeks to enhance the accuracy and efficiency of forecasting and optimization for PV-DG-ESS-grid hybrid plants in the region.

The objective of this study is to design a DE for a hybrid power plant of wind, solar, diesel engines, and ESS. When a utility requests ancillary services, the proposed dispatch engine would maximize resource use to account for any unusual changes in load circumstances. The DE will involve a combination of algorithms and models to predict the power output of each renewable energy source and optimize the dispatch of power between the different sources to meet the demand while minimizing costs and maximizing the use of renewable energy. 'Forecasting' and 'Real-time operator' are the two steps that make up the proposed DE. A long-term plan for the plant's operations throughout the next time period is what the first stage is meant to provide. The hybrid power plant can utilize this strategy to commit on an hourly basis to taking part in utility load sharing and the energy markets. The second stage will monitor plant operations and rearrange them in accordance with the current condition of the hybrid plant's parts.

With the use of the real load, PV, and wind data from a region in Sultanate of Oman, the suggested dispatch engine's feasibility has been evaluated. Oman's ambition to increase electricity production is to lessen its reliance on natural gas as a fuel source and support the new government fuel diversification program [65]. As stated in the Oman 2040 Vision, the development of unconventional sources employing natural resources, including as RE sources, would help lower production costs and improve a variety of economic sectors' competitiveness. The strategy aims to attain 20% of renewable energy consumption relative to overall consumption by 2030 and 35% to 39% by 2040 [66]. Therefore, implementing such a DE in Oman will be a great step toward the success of this plan.

The rest of the paper is structured as follows: Section 2 provides mathematical representations of the hybrid power system's component parts. The proposed Dispatch Engine (DE) is presented in Section 3. The model of the suggested system is developed in Sections 4, and the MILP approach is then introduced in Section 5. The forecasting method is described in Section 6. Section 7 presents the case simulation, while Section 8 presents the associated simulation findings. Finally, Section 10 provides the conclusions.

2. Proposed Hybrid System

Figure 1 depicts the functional block diagram of the proposed Dispatch Engine (DE). The proposed approach considers a microgrid consisting of a diesel generator (DG), a wind energy conversion system, a PV system, and an ESS system. The interconnection to a main grid and load for energy transfer is performed through a bidirectional inverter. Generally, RES, ESS and grid are interconnected via a DC bus facilitated by converters. This configuration allows for the ESS to be charged from the grid or the RES. Moreover, the ESS has the capability to release power to either the grid or loads.

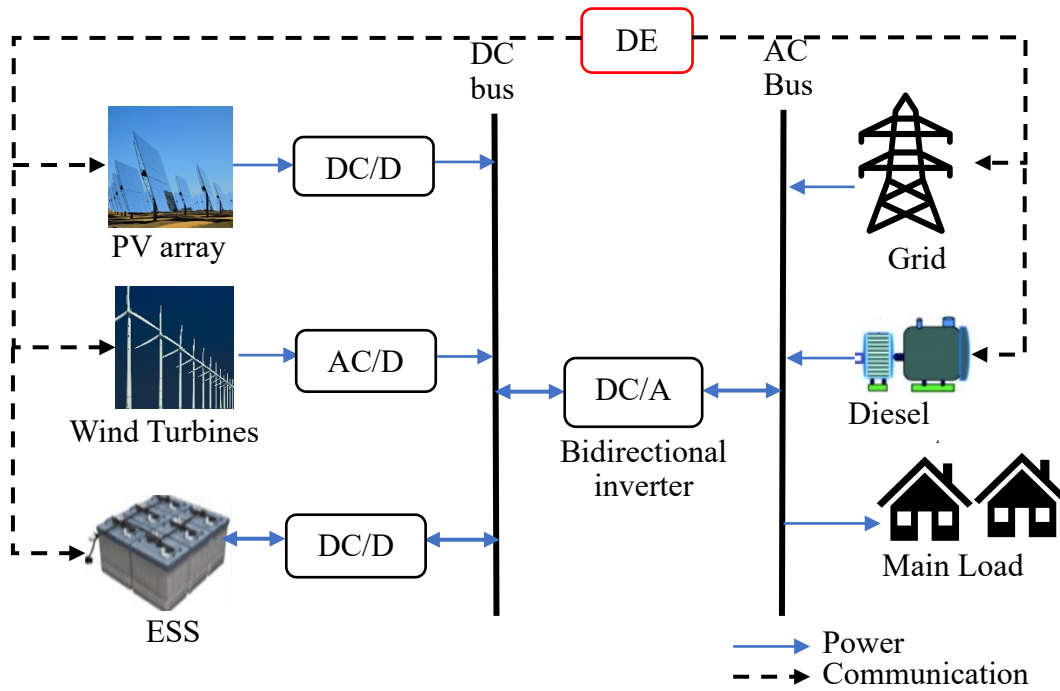


Figure 1. Dispatch Engine.

2.1. The ESS Model

Equations (1)–(5) may be used to compute the ESS's operation and State of Charge (SoC), subject to the limitations imposed by Equations (6)–(9), as shown below.

Discharge

$$E_{ESS}(t) = E_{ESS}(t-1) + P_{ESS}(t) \Delta t / \eta_{dis}, \quad P_{ESS}(t) = -ve \quad (1)$$

Charge

$$E_{ESS}(t) = E_{ESS}(t-1) + P_{ESS}(t) \Delta t \eta_{ch}, \quad P_{ESS}(t) = +ve \quad (2)$$

$$SoC = \frac{E_{ESS}(t)}{E_{ESS}^{max}} \quad (3)$$

Power limits:

$$P_{ESS}^{dis} \leq \frac{P_{ESS}(t)}{\eta_{dis}} \leq 0, \quad P_{ESS}(t) = -ve \quad (4)$$

$$0 \leq P_{ESS}(t) \eta_{ch} \leq P_{ESS}^{ch}, \quad P_{ESS}(t) = +ve \quad (5)$$

Storage energy limits

$$0 \leq E_{ESS}(t) \leq E_{ESS}^{max} \quad (6)$$

State of charge limits

$$SoC^{min} \leq SoC(t) \leq SoC^{max} \quad (7)$$

Starting operation of energy

$$E^{int} = \frac{SoC^{min}}{E_{ESS}^{max}} \quad (8)$$

Starting and ending of the state of charge

$$SoC^{int} = SoC^{end} \quad (9)$$

where P_{ESS} is the ESS's power output (MW), E_{ESS} is its stored energy (MWh), and Δt is the interval's time, which is equivalent to one hour. The discharge and charge efficiencies are denoted by η_{dis} and η_{ch} , respectively. The ESS's state of charge is represented by SoC, its maximum energy storage (MWh) by E_{ESS}^{max} , and its maximum charging and discharging powers (MW) by P_{ESS}^{ch} and P_{ESS}^{dis} , respectively. The state of charge's maximum and lower bounds are denoted by SoC^{max} and SoC^{min} , respectively. Positive and negative values are denoted by ve and $-ve$, respectively. E^{int} is the energy stored in the ESS at first (MWh), and SoC^{int} is the ESS's charge level at the end of the previous day. At the start of the day, SoC^{end} is the ESS state of charge [67].

2.2. PV Array Modeling

The proper connections of photovoltaic cells determine the output of the photovoltaic (PV) panels. PV cells are linked in series to create a string in order to give the necessary output voltage in the PV panel. Conversely, comparable strings are linked in parallel to boost a panel's output current capacity. This creates a PV panel or PV module, whose output power rating is calculated by multiplying the output side's voltage and current [68]. A number of models were created in [69] to calculate the PV panel output power, or P_{pv-out} . However, a straightforward model that accounts for two variables—ambient temperature and solar irradiance—has been employed in this investigation. This model's output power may be acquired as follows [70]:

$$P_{pv-out}(t) = P_{N-pv} \times \frac{G_t(t)}{G_{t-STC}} \times [1 + \alpha_t(T_c(t) - T_{c-STC})] \quad (10)$$

where P_{pv-out} is the PV module's output power (W); P_{N-pv} is its rated power (W) at standard test condition (STC), usually, the manufacturer specifies; G_t is the solar irradiance (W/m²); G_{t-STC} is the solar irradiance at STC ($G_{t-STC} = 1000$ W/m²); α_t is the temperature coefficient; T_{c-STC} is the cell temperature at STC ($T_{c-STC} = 25$ °); and T_c is the cell temperature (°C) [70].

2.3. Wind Turbine Modeling

The wind turbine generator's output power fluctuates in tandem with variations in wind speed, which is dependent on altitude at the same spot. As a result, the wind speed reported at the anemometer height needs to be corrected to the wind turbine's hub height [71]. In this case, the wind speed vertical profile of a given site is determined using two mathematical models, such as the log-law and the power law. The power-law model is used in this study to determine the wind profile, as shown below [70].

$$V_2 = V_1 \cdot \left(\frac{h_2}{h_1}\right)^\alpha \quad (11)$$

where V_1 (m/s) is the wind speeds at the anemometer and V_2 (m/s) is the wind speeds at hub height (h_1 (m) and h_2 (m)), and α is the power-law exponent. α is dependent on a number of variables, including temperature, wind speed, terrain roughness, height above ground, daytime hours, and season [70].

Based on the following equation, the wind turbine generator's output power may be assessed [70,72].

$$P_{wt}(t) = \begin{cases} 0 & V \leq V_{cut-in} \text{ or } V \geq V_{cut-out} \\ P_r \cdot \frac{V^3 - V_{cut-in}^3}{V_r^3 - V_{cut-in}^3} & V_{cut-in} < V < V_{rated} \\ P_r & V_{rated} < V < V_{cut-out} \end{cases} \quad (12)$$

where, V is the wind speed (m/s); P_r is the rated power (kW); and V_{cut-in} , V_{rated} , and $V_{cut-out}$ stand for the WT's cut-in, rated, and cut-out wind speeds, respectively, in m/s. The manufacturer often specifies these settings.

A wind turbine generator's rated power P_r (W) may be stated as a function of the air density p_{air} , the rated wind speed, the maximum power coefficient C_p , and the area swept by the blades.

$$P_r = \frac{1}{2} C_p \times p_{air} \times A_{wind} \times V_r^3 \quad (13)$$

2.4. Diesel Generator Modeling

According to literature calculated the fuel cost per year that the generator will need to operate during the system's lifetime as follows.

$$C_{DG} = C_F \times \sum_{t=1}^{8760} F(t) \quad (14)$$

where C_F is the unit fuel cost, $F(t)$ is the hourly fuel consumption of the generator, evaluated by:

$$F(t) = A \times P_{DG}(t) + B \times P_R \quad (15)$$

where $P_{DG}(t)$ is the power generated (KW) at time t , P_R is the rated power of the generator, A and B are the fuel curve coefficients.

In order to guarantee a constant supply of power to the load, the diesel generator is employed as a backup source when the energy from renewable energy sources (wind and PV) and batteries is unable to satisfy the demand, in other words

$$\frac{P_l(t)}{\eta_{inv}} > P_g(t) + [SOC(t-1) - (1 - DOD)] \times 1000 \times N_b \times C_b \quad (16)$$

Therefore, the needed power $P_{DG}(t)$ from the diesel generator is stated as follows:

$$P_{DG}(t) = P_l(t) - \{P_g(t) + [SOC(t-1) - (1 - DOD)] \times 1000 \times N_b \times C_b\} \times \eta_{inv} \quad (17)$$

If the needed power $P_{DG}(t)$ is more than the generator rated power of P_R , the loss of power supply (LPS) is computed by:

$$LPS = P_{DG}(t) - P_R \quad (18)$$

3. Dispatch Engine

By efficiently employing RESs and ESSs, the suggested DE in Figure 1 seeks to enhance hybrid plant profitability. In order to estimate the electricity demand, predict the power output of each renewable energy source, and optimize the dispatch of power between the various sources to meet the demand while minimizing costs and maximizing the use of renewable energy, the DE for a hybrid renewable power station would typically involve a combination of algorithms and models. Many data sources are accessible during the data analysis phase, including as the grid, RES stations, ESS data, and DG data.

The following actions would probably be included in the code for such a system:

- Data collection: Compile information on the historical and present electricity consumption, as well as the power production of each renewable energy source.
- Forecasting: Over the following several hours or days, estimate the power production of each renewable energy source and the amount of electricity that will be consumed using models and algorithms.
- Optimization: Employ algorithms for optimization to determine the best way to distribute electricity among the various sources in order to satisfy the anticipated demand while minimizing expenses and optimizing the usage of renewable energy. This may entail figuring out whether to utilize ESS or grid electricity, as well as the most effective mix of renewable energy sources to employ.
- Control: To maintain system stability and stay within operating parameters, use control algorithms to modify each source's output power in accordance with the dispatch plan.

Four different EMS will be employed in this study:

- Mode 1: In this mode, the load demand need is met by the generated electricity from renewable energy sources (PV and WT). The ESS is charged using the excess energy.
- Mode 2: When the ESS is completely charged, the power provided from renewable energy sources surpasses the load demand need. Here, the extra energy is sent to the grid.

- Mode 3: In this mode, the amount of electricity produced by renewable sources is insufficient to meet the demands of the load. In this instance, the ESS will make up the difference in power generation to meet the demands of the load.
- Mode 4: In this mode, the ESS level is low, and the electricity provided from renewable energy sources is insufficient to fulfill the load demand. In this situation, the system will draw the needed power from the grid. If the drawn power from the grid reaches its maximum allowed power to be drawn, the DG will run to make up for the shortfall in power supply to meet the demands of the load and further guarantee the ESS charge.

The suggested EMS algorithm flowchart utilized in the present research is displayed in Figure 2.

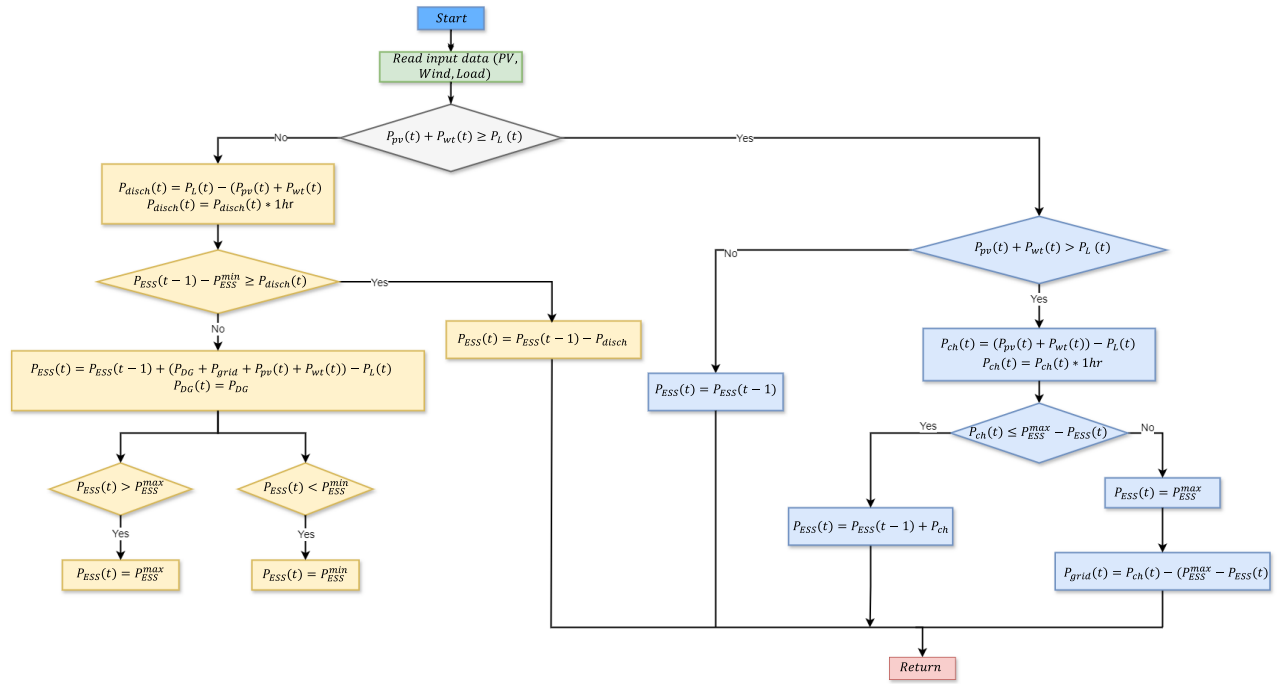


Figure 2. EMS algorithm flowchart.

4. Problem Formulation

Optimal outcomes are achieved through the identification of parameter settings that minimize a specific function, which in turn offers stakeholders a quantifiable insight into the system's value addition. To locate the function's minimum value, mathematical programming methods are frequently employed. These techniques navigate through predefined variables, aiming to find the optimal solution while adhering to a defined set of constraints. This process not only aids in optimizing system performance but also ensures that the solutions are feasible and aligned with the system's operational limits and goals. [73]. The problem can be described below:

$$\text{Find } X = \begin{Bmatrix} x_1 \\ x_1 \\ \vdots \\ x_n \end{Bmatrix} \text{ which minimizes } F(X) \quad (19)$$

Within constraints

$$\begin{aligned} g_j(x) &\leq 0, j=1, 2, \dots, m \\ l_j(x) &\leq 0, j=1, 2, \dots, p \end{aligned} \quad (20)$$

where $F(X)$, X , $g_j(x)$ and $l_j(x)$ are the objective function, n -dimensional design vector, inequality, and equality constraints, respectively. n is the number of variables and m and/or p are the numbers of constraints [73].

Various mathematical optimization techniques can be applied based on the problem's characteristics, especially in the context of renewable energy systems, which will be elaborated in the subsequent sections. The aforementioned DE has the primary goal of minimizing the costs of the hybrid plant and maximize the use of RES. To achieve this objective, each component relevant to the preceding statement needs to be precisely defined. Hence, the mathematical expression of the economic cost objective function C_{Total} can be formulated as

$$\min C_{Total} = C_{wind} + C_{PV} + C_{ESS} + C_{DG} + C_{grid} \quad (21)$$

where C_{Total} is the total cost function, C_{wind} is the cost function for wind power generation, C_{PV} is the cost function for PV power generation, C_{ESS} is the cost functions for the ESS, and C_{DG} is the cost functions for the DG, and C_{grid} is the grid cost functions. All cost functions in the model carry equal weightage, as the primary objective is to minimize the operating costs of the plants. Each cost function contributes to the same overarching goal and is of equal significance.

The cost functions for the DG (C_{DG}) is formulated as the aggregate of the fuel cost required for generating enough energy to meet grid demands and the associated emission costs. Given that CO2 accounts for around 99% of total emissions, the model overlooks the minor gases. With the mass of gases emitted from diesel combustion known, the emission cost can be quantified based on the amount of fuel consumed. Hence the cost function of DG can be expressed as

$$C_{DG} = \sum_{t=1}^{t+N} \Delta t \cdot \left(\frac{P_{DG}^G \cdot F}{P_{DG}^{max}} \cdot (C_f + C_m \alpha_{co_2}) \right) \quad \forall t \in [1, T] \quad (22)$$

where P_{DG}^G is the DG-generated power, F is the amount of diesel used per kWh, P_{DG}^{max} is the maximum power produced by DG, C_f the cost of fuel per liter, α_{co_2} is the gas mass associated with burning fuel and C_m is the cost of said gases.

The grid cost functions C_{grid} is defined as the difference between the cost of power purchased and the cost of power sold for each time interval.

The performance of the system is governed by a number of constraints on the proposed cost function. The power balance constraint is the first set of constraints that ensures at any time t , the total power generated from DG ($P_{DG,t}$), wind ($P_{wind,t}$), PV ($P_{PV,t}$), power imported or exported from or to the grid ($P_{grid,t}$) and power used for ESS ($P_{ESS,t}$) equals the total load power ($P_{L,t}$).

The power balance constraint is established as follows:

$$P_{PV,t} + P_{wind,t} + P_{ESS,t} + P_{DG,t} + P_{grid,t} = P_{L,t} \quad \forall t \in [1, T] \quad (23)$$

where $P_{PV,t}$ is the PV power, $P_{wind,t}$ is the wind power, $P_{ESS,t}$ is ESS power, $P_{DG,t}$ is the measured DG power, $P_{grid,t}$ is the grid power, and $P_{L,t}$ is load power and T is the operation time.

The second constraint is the generation limits constraint for the wind generators. The upper and lower limitations of the wind farm's output power are among the operating constraints [74].

$$0 \leq P_{wind,t} \leq P_{wind}^{max} \quad \forall t \in [1, T] \quad (24)$$

where P_{wind}^{max} is the maximum power output of the wind farm.

The third constrain is the generation limits constraint for the PV generators.

$$0 \leq P_{PV,t} \leq P_{PV}^{max} \quad \forall t \in [1, T] \quad (25)$$

where P_{PV}^{max} is the maximum power of the PV power station.

In order to balance the ESS's state of charge (SoC) throughout the charging and discharging cycles, a fourth constraints is established. The constraints of ESS include power capacity limits [74]

$$P_{ESS,min}(t) \leq P_{ESS}(t) \leq P_{ESS,max}(t), \quad \forall t \in [1, T] \quad (26)$$

where $P_{ESS,min}$ and $P_{ESS,max}$ are, respectively, the lower and upper limits of the ESS's power.

To prevent the ESS from being over-charged and over-discharged, its SoC limit is expressed as follows:

$$SoC_{min}(t) \leq SoC_{ESS}(t) \leq SoC_{max}(t), \quad \forall t \in [1, T] \quad (27)$$

where SoC_{min} and SoC_{max} are, respectively, the minimum and maximum bounds of SoC.

Capacity, charge and discharge power, and charge and discharge state constraints are some of the constraints placed on ESS. The following are the precise formulae.

$$\left\{ \begin{array}{ll} E^{min} \leq E_t \leq E^{max} & \forall t \in [1, T] \\ 0 \leq P_t^c \leq P^{c, max} & \forall t \in [1, T] \\ 0 \leq P_t^d \leq P^{d, max} & \forall t \in [1, T] \\ c_t + d_t \leq 1 & \forall t \in [1, T] \\ P_t = c_t P_t^c + d_t P_t^d & \forall t \in [1, T] \\ E_t = \frac{E_{t-1} + P_t^c \eta^c \Delta t - P_t^d \Delta t}{\eta^d} & \end{array} \right. \quad (28)$$

where E_t , E_{t-1} are the capacities of the ESS at time t and time $t-1$, E^{max} , E^{min} are the maximum and the minimum capacities of the ESS, P_t^c , P_t^d are the charge and discharge power of the ESS at time t , $P^{c, max}$, $P^{d, max}$ are the maximum charge power and the maximum discharge power of the ESS, c_t , d_t are the states of charge and discharge of the ESS at time t , $c_t=0$ means not charge of the ESS at time t , $c_t=1$ means charge of the ESS at time t , $d_t=0$ means not discharge of the ESS at time t , $d_t=1$ means discharge of the ESS at time t , η^c , η^d are the charge and the discharge efficiencies, respectively, and Δt is the unit time interval [75].

The fifth set of constraint is related to DG power and ensures that the generator limits are not exceeded. The upper and lower limitations of the output power are among the DG constraints.

$$0 \leq P_{DG,t} \leq P_{DG}^{max} \quad \forall t \in [1, T] \quad (29)$$

where P_{DG}^{max} is the DG unit's maximum power.

The last set of constraints is related to the maximum amount of power that may be transferred between the main grid and the microgrid. This power is limited between maximum and minimum values to ensure the system's transmission safety. Constraints include the output power's upper and lower limits, minimum power purchased, and the maximum power sold Equation (11).

$$P_{grid,min}(t) \leq P_{grid}(t) \leq P_{grid,max}(t), \quad \forall t \in [1, T] \quad (30)$$

where $P_{grid,max}$ and $P_{grid,min}$ is the grid's maximum and minimum power limits.

5. Mixed-Integer Linear Programming (MILP)

The Mixed-Integer Linear Programming (MILP) approach will be utilized to address the optimization issue presented in the preceding section. As such, this method follows the traditional MILP framework, focusing minimization. This approach is especially well-suited for optimizing complicated systems with several choice variables because of its ability to handle issues involving both discrete and continuous variables. Subject to a set of linear constraints, the research seeks to identify the most effective solution that minimizes the objective function by utilizing MILP. This method makes sure that the solution path is well-structured and also makes it easier to manage the many technical and operational limitations that are present in the optimization issue. Only c_t and d_t in ESS constraints are integers; all other arguments are real variables. Regarding the ESS's charging/discharging cycles' either/or behavior, the variables c_t and d_t are considered as binary (integer) variables.

Mixed-Integer Linear Programming (MILP) is a powerful mathematical optimization approach that finds the best solution within a feasible set using a well-defined objective function and a set of constraints. MILP stands out from other optimization tactics, such as classical linear programming, intelligent algorithms, and hybrid methods, due to its better precision and computing efficiency. This methodology's strength is its ability to efficiently include both discrete and continuous variables into the decision-making process, allowing for a thorough examination of complicated systems. The decision to use MILP as the selected optimization method for this study was due to its proved effectiveness of generating highly accurate solutions in a timely way, making it a useful tool for solving complex optimization difficulties [76].

To address MILP issues, three key strategies stand out for their effectiveness and efficiency: the feasibility pump technique, cutting edge methods, and tree search algorithms. The descriptions of those techniques are as below:

- The feasibility pump technique aims to quickly identify a viable solution that meets all issue constraints. It alternates between solving a relaxed linear problem to enhance objective value and rounding answers to retain feasibility under integer constraints. The feasibility pump is especially beneficial for quickly creating a viable starting point that may then be refined using other methods.
- Cutting Plane methods: These approaches, which rely on continually refining the viable solution space, apply extra constraints to remove regions that lack the optimal solution. These cuts are made with the solution of the linear relaxation of the MILP problem, which is gradually tightened to converge to the integer solution. This method is beneficial for reducing the search space and shortening the solution time for complex problems.
- Tree Search Algorithms: These algorithms, such as branch-and-bound and branch-and-cut, employ systematic exploration to identify viable solutions. They function by breaking down the solution space into smaller subproblems (branching) and assessing the limits of these subproblems to remove those that do not contain the optimal solution. Tree search algorithms are effective tools for tackling MILP issues because they can handle both the combinatorial character of integer variables and linear correlations between variables effectively.

Each of these techniques has distinct benefits and may be chosen based on the specific characteristics of the MILP issue at hand, such as its size, the nature of the constraints, and the desired balance of solution precision and computational time. Additionally, putting together these strategies or employing them in a planned sequence can considerably improve the efficiency of addressing MILP problems, leading the way for identifying ideal solutions in many applications [77].

The tree search technique, also known as branch-and-bound, is the approach that has been selected to solve the MILP issue. This approach is a crucial algorithmic method for solving MILP problems. Because of its architecture, it is possible to explore the solution space of MILP issues in a systematic way with the goal of precisely and effectively identifying the best or nearly optimal solution [77].

Using the MILP tree search approach, a search tree is constructed, with each node corresponding to a different subproblem inside the larger MILP framework. This procedure begins with the creation of a starting node that contains the full problem. It then branches depending on variables that must meet integer constraints to split the problem down into more manageable sub-problems. Figure 3 depicts an enumeration tree as the fundamental representation of the branch-and-bound method. A linear relaxation of the subproblem is carried out at each node in order to provide a lower bound for the ideal goal value. After branching, the algorithm uses linear programming to solve the relaxed linear version of each subproblem at the child nodes in order to get an upper bound for the ideal goal value. Bounding is an essential phase in the MILP tree search process that improves the search's efficiency and focus by fine-tuning the bounds using the output of linear programming relaxations. The search continues, gradually tightening its limits, until all nodes in the search tree have been explored or a predetermined stopping requirement is satisfied. The approach finds the best or nearly best possible integer solution to the initial MILP challenge through this painstaking search procedure, ultimately identifying the most efficient answer within the stated solution space [78].

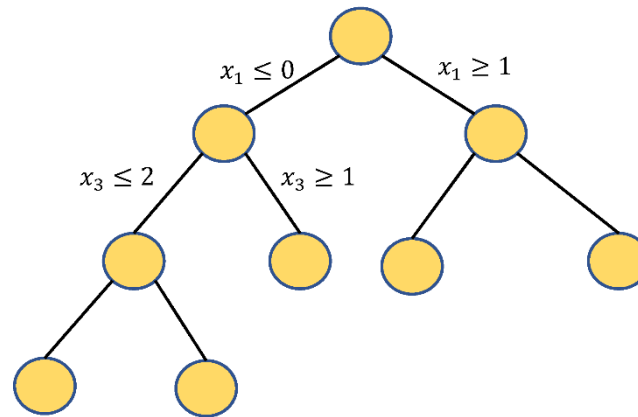


Figure 3. Branch-and-bound tree.

6. Wind, PV and Load Power Forecast

PV and wind energy are unpredictable and intermittent. It will affect the accuracy of the economic dispatch findings if the unpredictable data for wind and PV power are employed to solve the problem. In order to forecast wind and PV power, historical data must be used. Moreover, designing a robust and efficient EM that capitalizes on renewable energy sources necessitates a detailed and precise understanding of the load profile. The variability inherent in load profiles is a critical factor that influences the overall system reliability. Therefore, our research underscores the significance of precise load power forecasting to ensure the reliability and efficiency of energy management.

For effective PV, Wind, and load power forecasting, leveraging historical consumption data is imperative. By analyzing data from previous periods, neural networks can predict information for the future. Therefore, to forecast PV, Wind and Load power, neural networks are utilized [79,80]. These models are adept at interpreting complex data patterns, enabling them to predict future events based on historical data accurately.

Incorporating neural networks into our forecasting methodology is a cornerstone of our approach. With their ability to learn and adapt, neural networks offer a powerful tool for predicting future PV, Wind, and load power with high accuracy. This predictive capability is instrumental in optimizing the operation of renewable energy sources within the EMS, ensuring that energy supply aligns closely with demand patterns. Consequently, neural network-based forecasting represents a pivotal component of our strategy to enhance the efficiency and reliability of energy management in systems reliant on renewable energy sources [79,80].

6.1. Feed-Forward Neural Networks

In this study, we provide a feed-forward neural network (FFNN) based forecasting model. A neural network's architecture is made up of nodes, or neurons, arranged in three different levels, as shown in Figure 4: the input layer, one or more hidden layers, and the output layer. Weighted parameters are used to construct connections between nodes across these layers by measuring the strength of each link. The topology of the network produced by this arrangement is highly linked and replicates the structure of the biological nervous system. Every node in a layer is intimately connected to every other layer's node, creating a complete network that makes intricate data processing and pattern recognition jobs easier [81]. The input data is split 90:10 into training and testing sets before the network is trained using the Levenberg-Marquardt optimization approach. Data from the training and testing sets are used to validate the neural network model. After being trained, the network is then used to predict outputs for the input data that was used in the training and testing stages. The Mean Absolute Error (MAE) and the Root Mean Square Error (RMSE) for the training and testing datasets may be easily calculated according to this procedure, which compares expected and actual results [81].

The improved neural network model will be used to forecast future PV, wind, and load power over a 24-hour period. The input data for this prediction model comes from careful measurements made at several places throughout Oman. PV, wind, and load powers are monitored hourly to enable a thorough daily study. This results in the daily gathering of 24 different data points. With the help of this systemic method, daily PV, wind, and load power dynamics may be accurately represented, offering insightful information for energy management and planning.

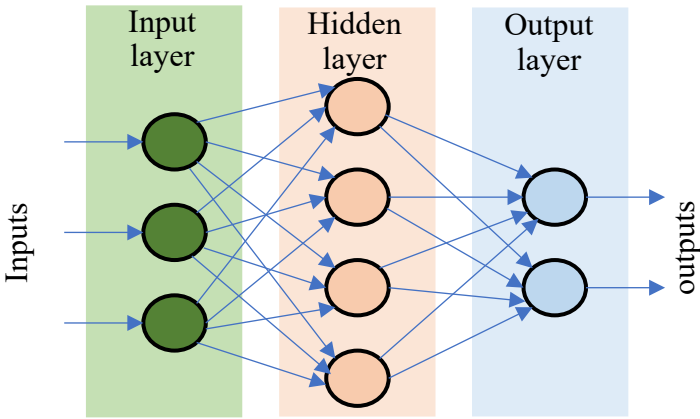


Figure 4. Feed-Forward Neural Networks (FFNN).

7. Case Simulation

The approach shown in Figure 1 is applied in the simulated scenario of this work. It consists of a microgrid with conventional (DG), a wind energy conversion system, photovoltaic (PV) system, and energy storage system (ESS).

The data used for Load, wind power and PV generation in this study come from the measurements from different locations in Oman. The cost coefficients for the generation of wind and PV electricity are shown in Table 3, which were collected from the reference [82]. Moreover, Table 3 presents the key features of the ESS. The mathematical model is solved using MILP, and wind and PV power generation are forecasted using a FFNN.

MATLAB is utilized for the implementation and simulation of the suggested method, as seen in Figure 1. The MATLAB Optimization Toolbox is used to tackle the optimization issue. In addition, the FFNN's capabilities are utilized for wind and solar power forecasting through the use of the MATLAB Neural Network Toolbox.

Table 3. System parameters.

Parameter	Value
Cost of solar power per kWh	0.048 \$
Cost of wind power per kWh	0.075 \$
Cost of DG power per kWh	0.34 \$
Cost of battery storage per kWh	0.22 \$
η^c	0.95
η^d	0.95
SoC^{min}	0.2
SoC^{max}	0.9
T	24 hours
Δt	1 hour

7.1. Load Data

Data on 2022's hourly load was given by the Oman Electricity Transmission Company (OETC) for one year. This dataset enabled an analysis of the daily load consumption patterns, which are

graphically represented in Figure 5. An examination of this data reveals a consistent trend where load consumption begins to decrease from 7:00 AM, reaching its lowest point between 7:00 AM and 9:00 AM. The load usage gradually rises after this trough and stays that way until 3:00 PM. The daily peak load is recorded around 9:00 PM, demonstrating a significant variance in power consumption throughout the day. The dynamics of power use are better understood thanks to this examination, which may also help develop more efficient supply and demand management techniques.

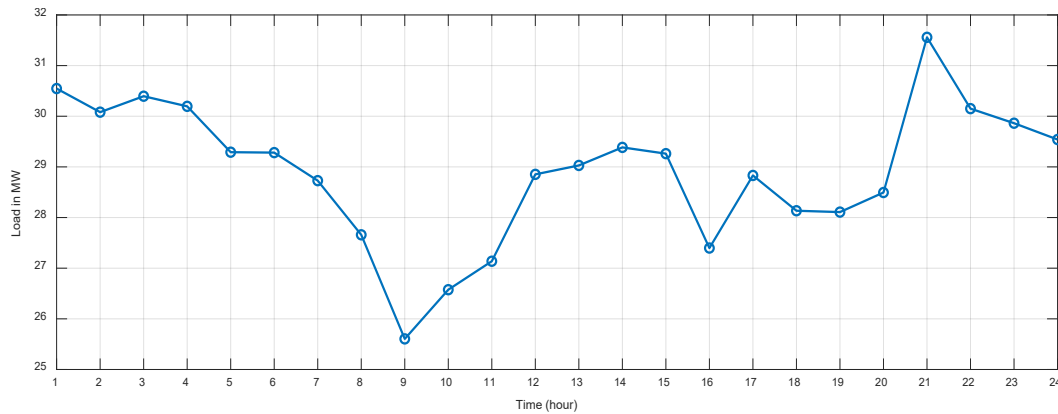


Figure 5. Load data.

The proposed Feed-Forward Neural Network (FFNN) is deployed to predict Load power utilizing historical electricity consumption data. This data is strategically partitioned into two distinct segments for the purposes of training and testing the model. Specifically, the initial 90% of the collected historical data sequence is allocated for the training phase of the FFNN model. During this phase, the network engages in a comprehensive analysis of the data, learning to identify underlying patterns and correlations that govern Load power fluctuations. This process equips the network with the ability to generate predictive insights based on historical trends.

The network does a thorough examination of the data during this phase in order to discover the underlying patterns and correlations that control variations in load power. By using past trends as a basis, this technique gives the network the capacity to produce predictive insights. After training, the remaining 10% of the data are used for the testing segment, which is a thorough assessment of the model's predictive power and performance. This stage is critical in determining how well the model can generalize its learnt patterns to new, unobserved data, which indicates how useful it will be in actual situations.

Within this testing methodology, the efficacy and precision of the FFNN in predicting load power are measured by contrasting the network's predictions with real observed data. This comparison aids in assessing how accurately and dependably the model captures the dynamics of load power usage.

The simulation results will be covered in depth in the following sections, along with a performance analysis of the FFNN model. These findings will demonstrate the model's effectiveness in predicting load power and highlight its potential use in improving energy management and planning techniques.

7.2. PV and Wind Data

The Oman Electricity Transmission Company (OETC) provided the wind power statistics utilized in this analysis, which were derived from measurements made in 2022. Oman Power and Water Procurement Company (OPWP) provided the PV data [83]. The PV and wind power data sets were both well documented at hourly intervals. With the help of this systematic process, a solid dataset consisting of 24 separate data points each day was gathered, which allowed for the capture of the power generation fluctuations throughout the day. Figure 6 shows the PV power data for a single day for visual reference. Figure 7 shows the wind power data for a single day and Figure 8

illustrates the wind power generation for 1 one month to indicate the nature of wind data. Notable variations in Figure 8 demonstrate how inconsistent the wind power data. This discrepancy will have an adverse effect on the FFNT training process and the wind power forecast accuracy.

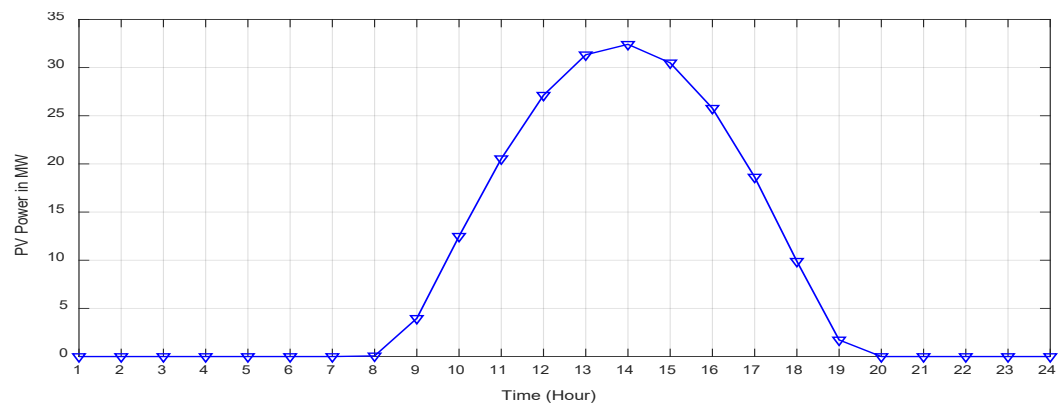


Figure 6. PV power data for one day.

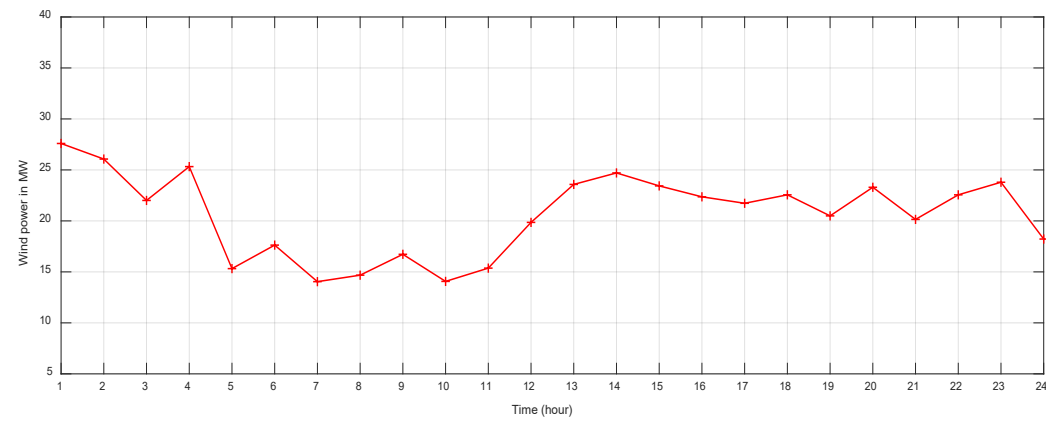


Figure 7. Wind power data for one day.

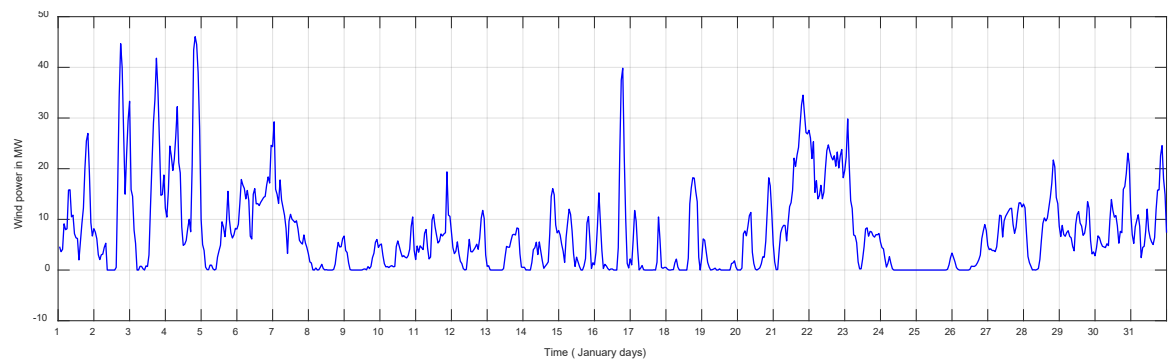


Figure 8. Wind power data for one month.

The suggested FFNN is used for forecasting PV and wind power data. The historical data sequence is divided into two sections: training and testing. In particular, the historical data sequence’s first 90% is set aside for the FF neural network model's training. The network may identify correlations and patterns in the data during this training phase. The trained model is subsequently tested using the remaining 10% of the data, enabling an evaluation of its generalization and predictive ability. The efficacy of the FFNN in forecasting wind power and PV may be determined by assessing

the network's accuracy on unobserved data. The next section presents the simulation results for the suggested FFNN model.

9. Results

9.1. Load Power Forecasting Results

Figure 9 presents the results of the forecast study and shows the estimated load power for a next 24-hour cycle. The graphical depiction provided by this figure provides a thorough breakdown of the expected fluctuations in load power throughout the course of the following day. By highlighting expected variations from one hour to the next, the representation effectively illustrates the anticipated load power dynamics. Better planning and management choices based on these forecast insights are made possible by this forecasting, which guarantees a thorough picture of the load power's expected behavior.

Furthermore, a thorough comparison of the "Actual" values—which represent the observed data—and the "Forecasted" values—which come from predictive analyses—is shown in Figure 9. The "Forecasted" curve closely resembles the size and path of the "Actual" curve, as can be seen by closely examining the curves in Figure 9. The remarkable resemblance between the two curves highlights the Feed-Forward Neural Network's (FFNN) great forecasting accuracy. The alignment shows how well the FFNN captures the complex patterns found in the real data, in addition to highlighting the model's capacity to forecast future trends. This comparison validates the FFNN's strong forecasting skills and highlights its potential as a dependable instrument for highly accurate load power prediction.

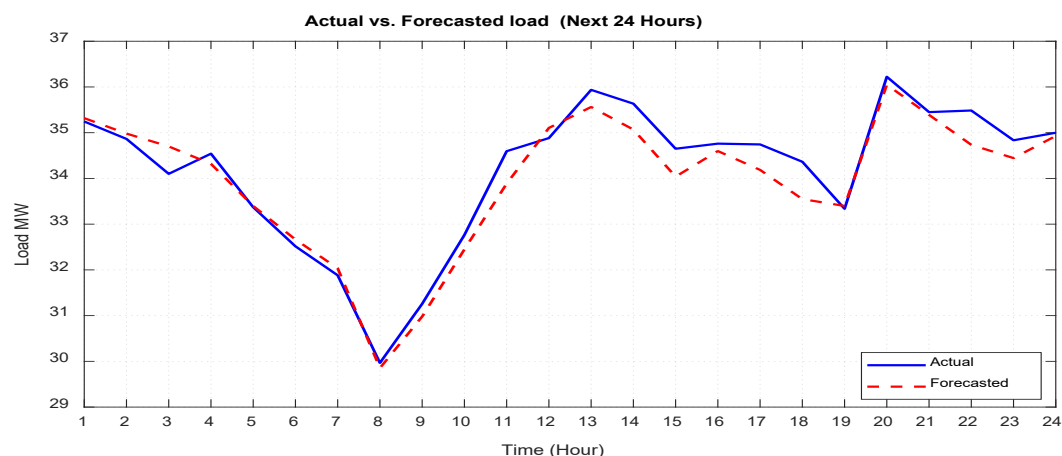


Figure 9. Forecast of wind power.

9.2. Wind and PV Power Forecasting Results

The expected values of the wind power for the next 24-hour period are graphically represented in Figure 10, which is one of the outputs of the forecasting phase, which is displayed in Figures 10 and 11. Similar to Figure 10, Figure 11 shows the predicted PV power generation and provides a visual representation of the forecasted PV output for an upcoming 24-hour period. The predicted data in this case starts and finishes on two distinct days at midnight.

A comparison between the "Actual" values, which show the actual data observed, and the "Forecasted" values, which show the results predicted, is displayed in Figures 9 and 10. It is clear by examining Figures 9 and 10's curves that the "Forecasted" curve accurately depicts the magnitude and trend of the "Actual" curve. The two curves' similarity shows that the FFNN has high forecasting capabilities. Additionally, the findings of wind power forecasting were shown to be not as precise as those of PV power forecasting. The nature of the two signals is responsible for this, due to the smoothness and slower rate of change of the PV data compared to the wind data. The accuracy of the

wind power forecast and the FFNT training procedure are negatively impacted by the previously indicated discrepancy in the wind data.

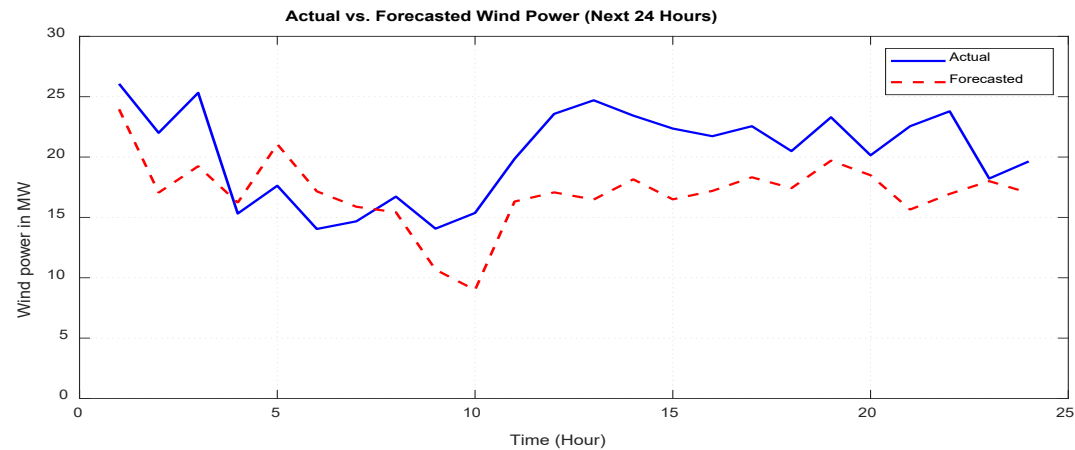


Figure 10. Forecast of wind power.

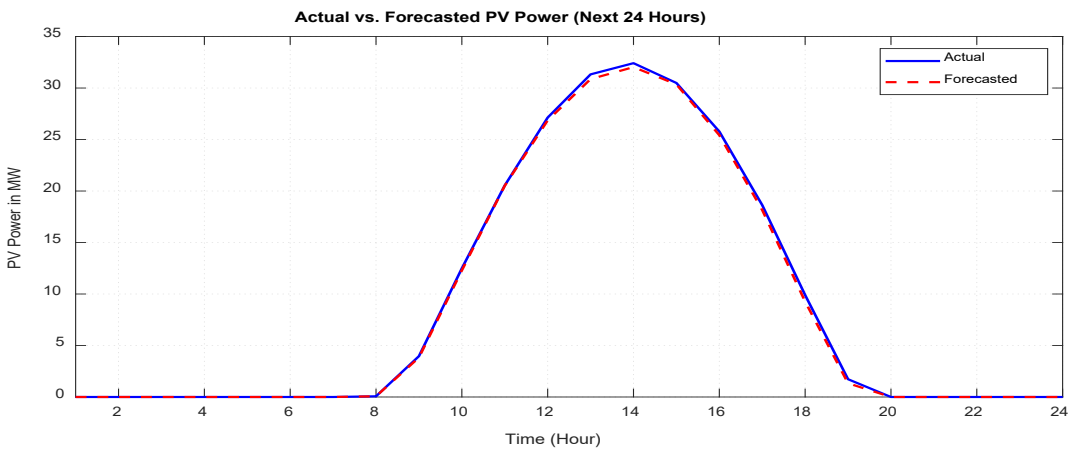


Figure 11. Forecast of PV power.

Furthermore, the suggested approach is compared with Long Short-Term Memory (LSTM) networks in order to evaluate the proposed FFNN. Where LSTM is an efficient way to manage sequences and time-dependent patterns, it is a specific kind of recurrent neural network (RNN). For PV power forecasting, the suggested technique and the LSTM proposed in [75] are tested. Figure 12 displays the simulation results for both approaches. Based on the simulation's output when LSTM was used to forecast PV power, the results were shown to be less accurate than when FFNN was used. Additionally, LSTM model training takes more time than the suggested FFNN. Furthermore, Table 4 displays a comparison between the standard deviations of the FFNN predictions, and LSTM predictions as well as the % difference between the standard deviations of the predictions and the actual data standard deviation. With the help of this comparison, it is possible to determine how much the variability in forecasts differs from the variability in the actual data. Notably, compared to the LSTM predictions, the FFNN forecasts had smaller standard deviation percentage differences. This result indicates that the FFNN model provides predictions with more consistency and accuracy.

Therefore, even though LSTMs are great at capturing distant relationships, which is crucial for time series forecasting. However, in our specific PV power forecast test, the LSTM model's performance fell short of the FFNN. As a result, the observed advantage of the FFNN model over the LSTM in our investigation emphasizes the significance of taking the issue domain as well as the data characteristics into account when choosing a forecasting approach. While LSTMs are praised for their sequence modeling skills, the FFNN model's ability to recognize complex patterns in the PV power

data allowed it to make predictions that were more accurate. In the end, the precise context and objectives of the prediction job will determine which approach to use FFNN or LSTM.

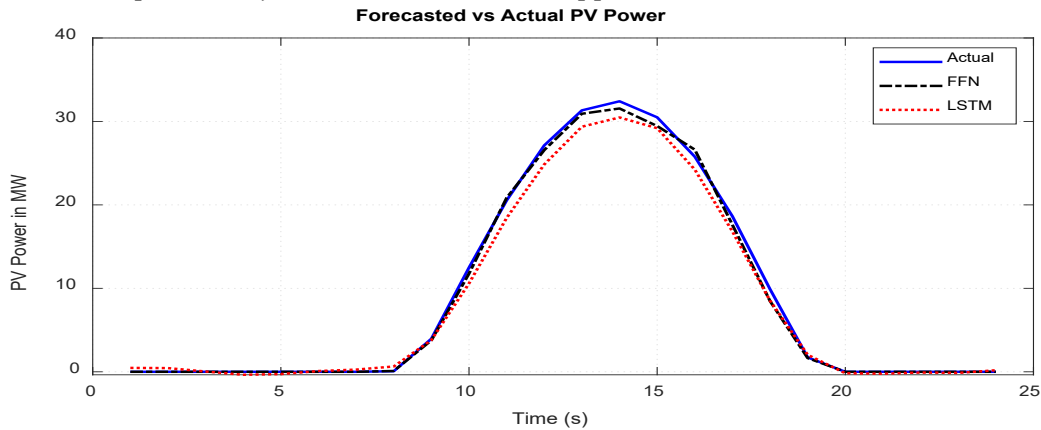


Figure 12. FFNN and LSTM Forecasting.

Table 4. Comparison between FFNN and LSTM.

Forecast Method	Prediction standard deviation	Percentage Difference from actual data standard deviation (12.3141)
FFNN	12.1647	-1.21%
LSTM	11.5562	-6.15%

9.2. Dispatch Engine Results

The problem of minimizing the cost in the energy dispatch of the micro-grid using DE, as depicted in Figure 1, has been successfully resolved. This solution is specific to the case study and relies on the utilization of the MILP solver. The results obtained from this approach, demonstrating the optimized energy dispatch and the corresponding minimum cost, are visually presented in Figure 13. Furthermore, the SOC% of the ESS is displayed throughout the day in Figure 14.

Figure 13 provides a visual representation of the contribution level of each generator element in the microgrid's energy supply. It illustrates the specific amount of energy that each generator element is required to generate in order to meet the overall energy demand. PV output begins at 8:00 AM and increases gradually until noon, when it peaks. Thereafter, it decreases until sunset. In contrast to PV, wind turbine production is unpredictable since it is based on the wind speed during each hour of the day. The wind generator begins to generate power if the wind speed is greater than the wind turbine's cut-in wind speed. The PV mostly meets the load demand at noon. The extra wind and PV power is sent to the grid and stored in ESS between the hours of 10:00 and 17:00 with a suitable amount of wind and PV energy output. When the wind and PV production is lower between the hours of 1:00 and 10:00 and 17:00 and 24:00, the grid and ESS are used to make up for the diminished wind and PV output. It can be observed that by employing this optimization strategy, the utilization of the DG unit is decreased, which lowers plant operating costs since the DG unit is only operated briefly. Additionally, by connecting the system to the grid, the grid will provide more output to compensate for the system's insufficient production from wind and PV energy, which will lower the rate at which wind power and PV will be curtailed.

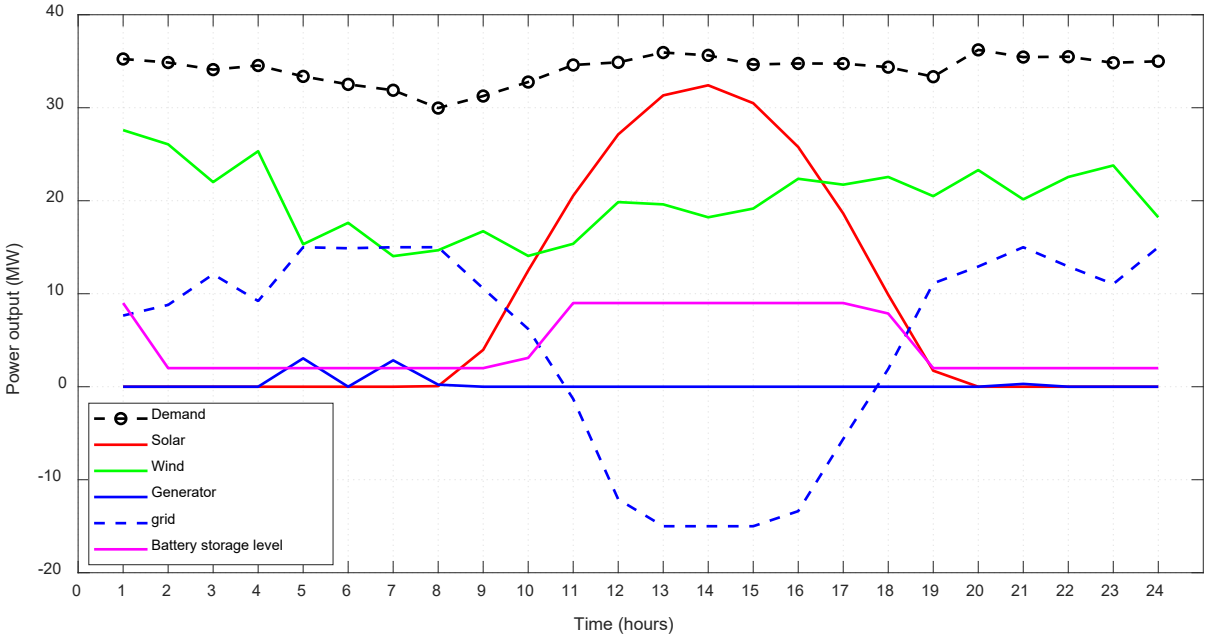


Figure 13. Dispatch of each generator with PV-Wind-DG-ESS-Grid hybrid plant.

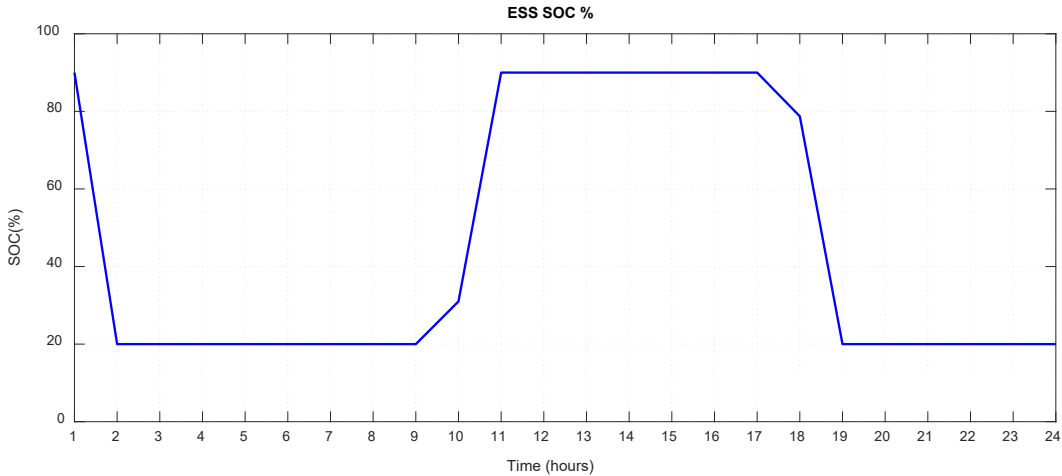


Figure 14. ESS SOC%.

To demonstrate how incorporating the grid affects system regulation performance a simulation is run for the designed DE utilizing a combination of PV, wind, DG, and ESS facilities. Figure 15 illustrates the variance in hybrid plant running costs between this scenario and the previous introduced. It is clear that when a system is disconnected from the grid, the DG unit is used more frequently, which raises plant operating costs since the system's insufficient output of wind and PV energy cannot be made up for by the grid.

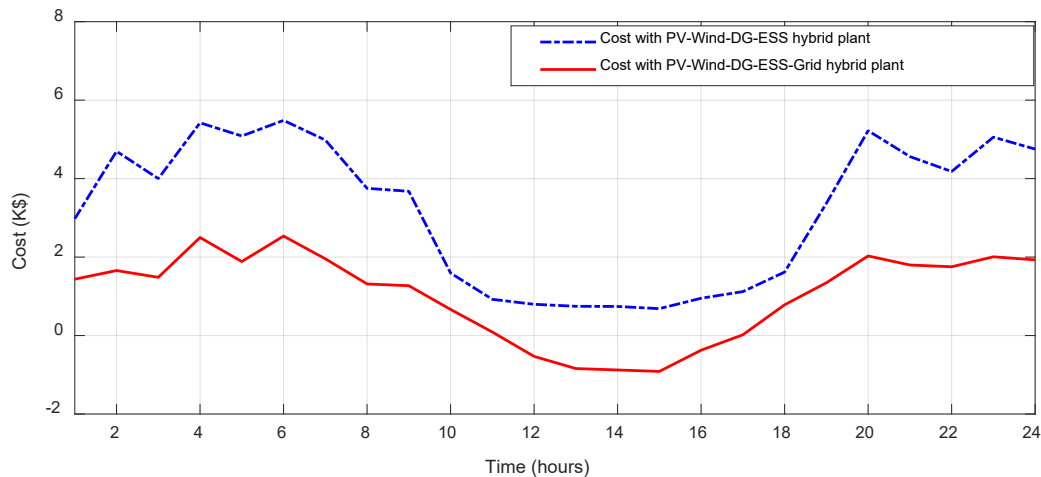


Figure 15. Hybrid plant operating costs for different optimal dispatch cases.

The suggested ED system, however, contains the ability to successfully support islanding operations in the context of real-time support conditions and auxiliary services for hybrid plant dispatch engines, according to the simulation that was given in this example. The proposed ED system has proven its capacity to enable a smooth transition to islanded operation in the case of grid failures or maintenance by tightly integrating advanced control algorithms and responsive data analytics. This accomplishment shows how reliable the proposed strategy is in preserving grid stability and power supply continuity, adding to the necessary range of ancillary services that contemporary hybrid plant dispatch engines work to provide.

10. Conclusions

In order to ensure dispatchable electricity under challenging operating conditions, hybrid power plants have emerged as dependable and adaptable electricity producing facilities. In order to design and run hybrid power plants, this research suggests implementing a dispatch engine (DE) based on mixed-integer linear programming (MILP). The DE seeks to minimize operating costs and the reliance on diesel generators (DGs) while maintaining the agreed energy output by offering extended duration operating schedules and facilitating real-time monitoring. The recommended approach includes accurate PV and wind power forecasts, ensuring the best possible scheduling. To assess the feasibility of the proposed dispatch engine a case study is conducted in Oman, utilizing real-time data from multiple sites in the country on load, wind power, and PV power. Using a hybrid PV-Wind-DG-ESS-Grid plant, the proposed dispatch engine's performance is assessed, offering helpful insights into the possible advantages and efficiency of the suggested system. The Feed-Forward (FF) neural network is used to forecast data for Load, PV and wind power, and the findings demonstrate the strong forecasting capabilities of the FF neural network. The implementation results of the proposed DE show how wind and PV energy is sent to the grid and stored in ESS during peak hours. When production decreases, the grid and ESS compensate. Moreover, the simulation results show that using the proposed DE reduces DG unit usage and lowers plant operating costs.

Author Contributions: Methodology, M.S., R.A.A. and H.Y.; Software, M.S.; Validation, R.A.A., H.Y.; Writing—original draft preparation, M.S.; Supervision, R.A.A., H.Y.; Writing—review and editing, R.A.A., H.Y. All authors have read and agreed to the published version of the manuscript.

Funding: This research is sponsored by a collaborative fund between Sultan Qaboos University and Qatar University, with the code number CL/SQU-QU/SERC/22/01. The research title is "Design and Implementation of an Intelligent Dispatch Engine for Hybrid Renewable Power Stations."

Acknowledgments: The authors would like to thank Oman Electricity Transmission Company (OETC), Oman, for providing the data and required information about the study.

Conflicts of Interest: The authors declare no conflict of interest.

Abbreviations

DE	Dispatch engine
DGs	Diesel generators
DP	Dynamic programming
ED	Economic dispatch
ESS	Energy storage systems
FFNN	Feed-forward neural networks
HRES	Hybrid renewable energy system
LCOE	Levelized Cost of Electricity
LPM	Linear programming model
LPS	loss of power supply
LSTM	Long short-term memory
MCGP	Multi choice goal programming
MILP	Mixed integer linear programming
MOEA	Multi-objective evolutionary algorithms
NLP	Nonlinear programming
PCC	Point of common coupling
PSO	Particle swarm optimization
PV	Photovoltaic
RE	Renewable energy
RNN	Recurrent neural network
RTED	Real-time economic dispatch
SoC	State of Charge

References

1. T. Kober, H.-W. Schiffer, M. Densing, and E. Panos, "Global energy perspectives to 2060–WEC's World Energy Scenarios 2019," *Energy Strategy Reviews*, vol. 31, p. 100523, 2020.
2. M. F. Ishraque, S. A. Shezan, M. Ali, and M. Rashid, "Optimization of load dispatch strategies for an islanded microgrid connected with renewable energy sources," *Applied Energy*, vol. 292, p. 116879, 2021.
3. Y. Mohammed, M. Mustafa, and N. Bashir, "Hybrid renewable energy systems for off-grid electric power: Review of substantial issues," *Renewable and Sustainable Energy Reviews*, vol. 35, pp. 527-539, 2014.
4. F. Katiraei, R. Iravani, N. Hatziargyriou, and A. Dimeas, "Microgrids management," *IEEE power and energy magazine*, vol. 6, pp. 54-65, 2008.
5. P. Bajpai and V. Dash, "Hybrid renewable energy systems for power generation in stand-alone applications: A review," *Renewable and Sustainable Energy Reviews*, vol. 16, pp. 2926-2939, 2012.
6. S. Mandal, B. K. Das, and N. Hoque, "Optimum sizing of a stand-alone hybrid energy system for rural electrification in Bangladesh," *Journal of Cleaner Production*, vol. 200, pp. 12-27, 2018.
7. M. Baneshi and F. Hadianfard, "Techno-economic feasibility of hybrid diesel/PV/wind/battery electricity generation systems for non-residential large electricity consumers under southern Iran climate conditions," *Energy Conversion and Management*, vol. 127, pp. 233-244, 2016.
8. M. Mehrpooya, M. Mohammadi, and E. Ahmadi, "Techno-economic-environmental study of hybrid power supply system: A case study in Iran," *Sustainable Energy Technologies and Assessments*, vol. 25, pp. 1-10, 2018.
9. S. A. Shezan, S. Julai, M. Kibria, K. Ullah, R. Saidur, W. Chong, et al., "Performance analysis of an off-grid wind-PV (photovoltaic)-diesel-battery hybrid energy system feasible for remote areas," *Journal of Cleaner Production*, vol. 125, pp. 121-132, 2016.
10. S. M. Hosseini, R. Carli, and M. Dotoli, "Robust optimal energy management of a residential microgrid under uncertainties on demand and renewable power generation," *IEEE Transactions on Automation Science and Engineering*, vol. 18, pp. 618-637, 2020.
11. S. Kakran and S. Chanana, "Smart operations of smart grids integrated with distributed generation: A review," *Renewable and Sustainable Energy Reviews*, vol. 81, pp. 524-535, 2018.
12. K. Utkarsh, D. Srinivasan, A. Trivedi, W. Zhang, and T. Reindl, "Distributed model-predictive real-time optimal operation of a network of smart microgrids," *IEEE Transactions on Smart Grid*, vol. 10, pp. 2833-2845, 2018.

13. B.-Y. Qu, Y. Zhu, Y. Jiao, M. Wu, P. N. Suganthan, and J. J. Liang, "A survey on multi-objective evolutionary algorithms for the solution of the environmental/economic dispatch problems," *Swarm and Evolutionary Computation*, vol. 38, pp. 1-11, 2018.
14. G. Xiong, D. Shi, and X. Duan, "Multi-strategy ensemble biogeography-based optimization for economic dispatch problems," *Applied energy*, vol. 111, pp. 801-811, 2013.
15. M. Ellahi, G. Abbas, I. Khan, P. M. Koola, M. Nasir, A. Raza, et al., "Recent approaches of forecasting and optimal economic dispatch to overcome intermittency of wind and photovoltaic (PV) systems: A review," *Energies*, vol. 12, p. 4392, 2019.
16. H. Xia, Q. Li, R. Xu, T. Chen, J. Wang, M. A. S. Hassan, et al., "Distributed control method for economic dispatch in islanded microgrids with renewable energy sources," *IEEE Access*, vol. 6, pp. 21802-21811, 2018.
17. Z. Tang, D. J. Hill, and T. Liu, "A novel consensus-based economic dispatch for microgrids," *IEEE Transactions on Smart Grid*, vol. 9, pp. 3920-3922, 2018.
18. S. Yang, S. Tan, and J.-X. Xu, "Consensus based approach for economic dispatch problem in a smart grid," *IEEE Transactions on Power Systems*, vol. 28, pp. 4416-4426, 2013.
19. S. S. Reddy, P. Bijwe, and A. R. Abhyankar, "Real-time economic dispatch considering renewable power generation variability and uncertainty over scheduling period," *IEEE Systems journal*, vol. 9, pp. 1440-1451, 2014.
20. K. M. Muttaqi and D. Sutanto, "An effective power dispatch strategy to improve generation schedulability by mitigating wind power uncertainty with a data driven flexible dispatch margin for a wind farm using a multi-unit battery energy storage system," in *2018 IEEE Industry Applications Society Annual Meeting (IAS)*, 2018, pp. 1-8.
21. L. Ye, C. Zhang, Y. Tang, W. Zhong, Y. Zhao, P. Lu, et al., "Hierarchical model predictive control strategy based on dynamic active power dispatch for wind power cluster integration," *IEEE Transactions on Power Systems*, vol. 34, pp. 4617-4629, 2019.
22. S. S. Arefin, "Optimization techniques of islanded hybrid microgrid system," in *Renewable Energy-Resources, Challenges and Applications*, ed: IntechOpen, 2020.
23. A. Chauhan and R. Saini, "A review on Integrated Renewable Energy System based power generation for stand-alone applications: Configurations, storage options, sizing methodologies and control," *Renewable and Sustainable Energy Reviews*, vol. 38, pp. 99-120, 2014.
24. M. Husein and I.-Y. Chung, "Optimal design and financial feasibility of a university campus microgrid considering renewable energy incentives," *Applied energy*, vol. 225, pp. 273-289, 2018.
25. S. Mazzola, M. Astolfi, and E. Macchi, "The potential role of solid biomass for rural electrification: A techno economic analysis for a hybrid microgrid in India," *Applied Energy*, vol. 169, pp. 370-383, 2016.
26. S. Mazzola, C. Vergara, M. Astolfi, V. Li, I. Perez-Arriaga, and E. Macchi, "Assessing the value of forecast-based dispatch in the operation of off-grid rural microgrids," *Renewable Energy*, vol. 108, pp. 116-125, 2017.
27. L. Moretti, M. Astolfi, C. Vergara, E. Macchi, J. I. Pérez-Arriaga, and G. Manzolini, "A design and dispatch optimization algorithm based on mixed integer linear programming for rural electrification," *Applied energy*, vol. 233, pp. 1104-1121, 2019.
28. L. Ferrer-Martí, B. Domenech, A. García-Villoria, and R. Pastor, "A MILP model to design hybrid wind-photovoltaic isolated rural electrification projects in developing countries," *European Journal of Operational Research*, vol. 226, pp. 293-300, 2013.
29. E. D. Mehleri, H. Sarimveis, N. C. Markatos, and L. G. Papageorgiou, "Optimal design and operation of distributed energy systems: Application to Greek residential sector," *Renewable Energy*, vol. 51, pp. 331-342, 2013.
30. L. Moretti, S. Polimeni, L. Meraldi, P. Raboni, S. Leva, and G. Manzolini, "Assessing the impact of a two-layer predictive dispatch algorithm on design and operation of off-grid hybrid microgrids," *Renewable Energy*, vol. 143, pp. 1439-1453, 2019.
31. A. G. Dagnachew, P. L. Lucas, A. F. Hof, D. E. Gernaat, H.-S. de Boer, and D. P. van Vuuren, "The role of decentralized systems in providing universal electricity access in Sub-Saharan Africa—A model-based approach," *Energy*, vol. 139, pp. 184-195, 2017.
32. H.-H. Renewable, "Distributed Generation System Design Software," URL <http://homerenergy.com>, 2017.
33. C. D. Barley and C. B. Winn, "Optimal dispatch strategy in remote hybrid power systems," *Solar Energy*, vol. 58, pp. 165-179, 1996.

34. E. Eriksson and E. M. Gray, "Optimization and integration of hybrid renewable energy hydrogen fuel cell energy systems—A critical review," *Applied energy*, vol. 202, pp. 348-364, 2017.
35. C. Ammari, D. Belatrache, B. Touhami, and S. Makhloufi, "Sizing, optimization, control and energy management of hybrid renewable energy system—A review," *Energy and Built Environment*, 2021.
36. M. D. Al-Falahi, S. Jayasinghe, and H. Enshaei, "A review on recent size optimization methodologies for standalone solar and wind hybrid renewable energy system," *Energy conversion and management*, vol. 143, pp. 252-274, 2017.
37. R. Siddaiah and R. Saini, "A review on planning, configurations, modeling and optimization techniques of hybrid renewable energy systems for off grid applications," *Renewable and Sustainable Energy Reviews*, vol. 58, pp. 376-396, 2016.
38. M. Vaccari, G. Mancuso, J. Riccardi, M. Cantù, and G. Pannocchia, "A sequential linear programming algorithm for economic optimization of hybrid renewable energy systems," *Journal of process control*, vol. 74, pp. 189-201, 2019.
39. C.-T. Chang, "Multi-choice goal programming model for the optimal location of renewable energy facilities," *Renewable and Sustainable Energy Reviews*, vol. 41, pp. 379-389, 2015.
40. M. Ming, R. Wang, Y. Zha, and T. Zhang, "Multi-objective optimization of hybrid renewable energy system using an enhanced multi-objective evolutionary algorithm," *Energies*, vol. 10, p. 674, 2017.
41. R. Wang, G. Li, M. Ming, G. Wu, and L. Wang, "An efficient multi-objective model and algorithm for sizing a stand-alone hybrid renewable energy system," *Energy*, vol. 141, pp. 2288-2299, 2017.
42. M. Nemati, M. Braun, and S. Tenbohlen, "Optimization of unit commitment and economic dispatch in microgrids based on genetic algorithm and mixed integer linear programming," *Applied energy*, vol. 210, pp. 944-963, 2018.
43. N. Wu and H. Wang, "Deep learning adaptive dynamic programming for real time energy management and control strategy of micro-grid," *Journal of cleaner production*, vol. 204, pp. 1169-1177, 2018.
44. B. Das and A. Kumar, "A NLP approach to optimally size an energy storage system for proper utilization of renewable energy sources," *Procedia Computer Science*, vol. 125, pp. 483-491, 2018.
45. A. Derrouazin, M. Aillerie, N. Mekakia-Maaza, and J.-P. Charles, "Multi input-output fuzzy logic smart controller for a residential hybrid solar-wind-storage energy system," *Energy Conversion and Management*, vol. 148, pp. 238-250, 2017.
46. L. Suganthi, S. Iniyan, and A. A. Samuel, "Applications of fuzzy logic in renewable energy systems—a review," *Renewable and sustainable energy reviews*, vol. 48, pp. 585-607, 2015.
47. M. Athari and M. Ardehali, "Operational performance of energy storage as function of electricity prices for on-grid hybrid renewable energy system by optimized fuzzy logic controller," *Renewable Energy*, vol. 85, pp. 890-902, 2016.
48. S. M. Mahmoudi, A. Maleki, and D. R. Ochbelagh, "Optimization of a hybrid energy system with/without considering back-up system by a new technique based on fuzzy logic controller," *Energy Conversion and Management*, vol. 229, p. 113723, 2021.
49. M. J. Mayer, A. Szilágyi, and G. Gróf, "Environmental and economic multi-objective optimization of a household level hybrid renewable energy system by genetic algorithm," *Applied Energy*, vol. 269, p. 115058, 2020.
50. B. K. Das, R. Hassan, M. S. H. Tushar, F. Zaman, M. Hasan, and P. Das, "Techno-economic and environmental assessment of a hybrid renewable energy system using multi-objective genetic algorithm: A case study for remote Island in Bangladesh," *Energy Conversion and Management*, vol. 230, p. 113823, 2021.
51. A. Abdelkader, A. Rabeh, D. M. Ali, and J. Mohamed, "Multi-objective genetic algorithm based sizing optimization of a stand-alone wind/PV power supply system with enhanced battery/supercapacitor hybrid energy storage," *Energy*, vol. 163, pp. 351-363, 2018.
52. X. Lü, Y. Wu, J. Lian, Y. Zhang, C. Chen, P. Wang, et al., "Energy management of hybrid electric vehicles: A review of energy optimization of fuel cell hybrid power system based on genetic algorithm," *Energy Conversion and Management*, vol. 205, p. 112474, 2020.
53. M. S. Javed, A. Song, and T. Ma, "Techno-economic assessment of a stand-alone hybrid solar-wind-battery system for a remote island using genetic algorithm," *Energy*, vol. 176, pp. 704-717, 2019.

54. M. M. Rahman, M. Shakeri, S. K. Tiong, F. Khatun, N. Amin, J. Pasupuleti, et al., "Prospective methodologies in hybrid renewable energy systems for energy prediction using artificial neural networks," *Sustainability*, vol. 13, p. 2393, 2021.
55. S. Amirtharaj, L. Premalatha, and D. Gopinath, "Optimal utilization of renewable energy sources in MG connected system with integrated converters: An AGONN Approach," *Analog Integrated Circuits and Signal Processing*, vol. 101, pp. 513-532, 2019.
56. M. Azaza and F. Wallin, "Multi objective particle swarm optimization of hybrid micro-grid system: A case study in Sweden," *Energy*, vol. 123, pp. 108-118, 2017.
57. C. Shang, D. Srinivasan, and T. Reindl, "An improved particle swarm optimisation algorithm applied to battery sizing for stand-alone hybrid power systems," *International Journal of Electrical Power & Energy Systems*, vol. 74, pp. 104-117, 2016.
58. A. Elsheikh and M. Abd Elaziz, "Review on applications of particle swarm optimization in solar energy systems," *International Journal of Environmental Science and Technology*, vol. 16, pp. 1159-1170, 2019.
59. G. Zhang, B. Wu, A. Maleki, and W. Zhang, "Simulated annealing-chaotic search algorithm based optimization of reverse osmosis hybrid desalination system driven by wind and solar energies," *Solar Energy*, vol. 173, pp. 964-975, 2018.
60. W. Zhang, A. Maleki, M. A. Rosen, and J. Liu, "Sizing a stand-alone solar-wind-hydrogen energy system using weather forecasting and a hybrid search optimization algorithm," *Energy conversion and management*, vol. 180, pp. 609-621, 2019.
61. W. Zhang, A. Maleki, M. A. Rosen, and J. Liu, "Optimization with a simulated annealing algorithm of a hybrid system for renewable energy including battery and hydrogen storage," *Energy*, vol. 163, pp. 191-207, 2018.
62. Y. Gu, X. Zhang, J. A. Myhren, M. Han, X. Chen, and Y. Yuan, "Techno-economic analysis of a solar photovoltaic/thermal (PV/T) concentrator for building application in Sweden using Monte Carlo method," *Energy Conversion and Management*, vol. 165, pp. 8-24, 2018.
63. N. Ghorbani, A. Kasaeian, A. Toopshekan, L. Bahrani, and A. Maghami, "Optimizing a hybrid wind-PV-battery system using GA-PSO and MOPSO for reducing cost and increasing reliability," *Energy*, vol. 154, pp. 581-591, 2018.
64. A. Heydari, D. A. Garcia, F. Keynia, F. Bisegna, and L. De Santoli, "A novel composite neural network based method for wind and solar power forecasting in microgrids," *Applied Energy*, vol. 251, p. 113353, 2019.
65. O. s.-Y. S.-. Oman Power and Water Procurement, " 2019. and [Online].
66. O. V. D. Oman 2040 Vision Office, " 2019.
67. K. Borisoot, R. Liemthong, C. Srithapon, and R. Chatthaworn, "Optimal energy management for virtual power plant considering operation and degradation costs of energy storage system and generators," *Energies*, vol. 16, p. 2862, 2023.
68. A. Fathy, K. Kaaniche, and T. M. Alanazi, "Recent approach based social spider optimizer for optimal sizing of hybrid PV/wind/battery/diesel integrated microgrid in aljouf region," *IEEE Access*, vol. 8, pp. 57630-57645, 2020.
69. R. Ayop and C. W. Tan, "A comprehensive review on photovoltaic emulator," *Renewable and Sustainable Energy Reviews*, vol. 80, pp. 430-452, 2017.
70. Z. Belboul, B. Toual, A. Kouzou, L. Mokrani, A. Bensalem, R. Kennel, et al., "Multiobjective optimization of a hybrid PV/Wind/Battery/Diesel generator system integrated in microgrid: A case study in Djelfa, Algeria," *Energies*, vol. 15, p. 3579, 2022.
71. O. Nadjemi, T. Nacer, A. Hamidat, and H. Salhi, "Optimal hybrid PV/wind energy system sizing: Application of cuckoo search algorithm for Algerian dairy farms," *Renewable and Sustainable Energy Reviews*, vol. 70, pp. 1352-1365, 2017.
72. W. Dong, Y. Li, and J. Xiang, "Optimal sizing of a stand-alone hybrid power system based on battery/hydrogen with an improved ant colony optimization," *Energies*, vol. 9, p. 785, 2016.
73. S. S. Rao, *Engineering optimization: theory and practice*: John Wiley & Sons, 2019.
74. Y. Hu, Y. Li, M. Xu, L. Zhou, and M. Cui, "A chance-constrained economic dispatch model in wind-thermal-energy storage system," *Energies*, vol. 10, p. 326, 2017.
75. X. Liu, X. Li, J. Tian, Y. Wang, G. Xiao, and P. Wang, "Day-Ahead Economic Dispatch of Renewable Energy System considering Wind and Photovoltaic Predicted Output," *International Transactions on Electrical Energy Systems*, vol. 2022, 2022.

76. J. Ma and X. Ma, "A review of forecasting algorithms and energy management strategies for microgrids," *Systems Science & Control Engineering*, vol. 6, pp. 237-248, 2018.
77. J. P. Vielma, "Mixed integer linear programming formulation techniques," *Siam Review*, vol. 57, pp. 3-57, 2015.
78. J. C. Smith and Z. C. Taskin, "A tutorial guide to mixed-integer programming models and solution techniques," *Optimization in Medicine and Biology*, pp. 521-548, 2008.
79. Y. Ren, P. Suganthan, and N. Srikanth, "Ensemble methods for wind and solar power forecasting—A state-of-the-art review," *Renewable and Sustainable Energy Reviews*, vol. 50, pp. 82-91, 2015.
80. M. Abuelma and B. Chowdhury, "Solar power forecasting using artificial neural networks," in *2015 North American Power Symposium (NAPS)*, 2015, pp. 1-5.
81. V. Sharma, S. Rai, and A. Dev, "A comprehensive study of artificial neural networks," *International Journal of Advanced research in computer science and software engineering*, vol. 2, 2012.
82. I. R. E. A. (IRENA). (2021). Available: <https://www.irena.org/Energy-Transition/Technology/Power-generation-costs>
83. O. P. a. W. P. C. (OPWP). Available: <https://omanpwp.om/new/Documents.aspx?Pid=84>

Disclaimer/Publisher's Note: The statements, opinions and data contained in all publications are solely those of the individual author(s) and contributor(s) and not of MDPI and/or the editor(s). MDPI and/or the editor(s) disclaim responsibility for any injury to people or property resulting from any ideas, methods, instructions or products referred to in the content.